

# Anharmonicity and self-energy effects of the $E_{2g}$ phonon in $\text{MgB}_2$

A. Mialitsin<sup>1,†</sup>, B. S. Dennis<sup>1</sup>, N. D. Zhigadlo<sup>2</sup>, J. Karpinski<sup>2</sup>, and G. Blumberg<sup>1,\*</sup>

<sup>1</sup>*Bell Laboratories, Alcatel-Lucent, Murray Hill, NJ 07974*

<sup>2</sup>*Solid State Physics Lab, ETH, CH-8093 Zürich, Switzerland*

<sup>†</sup>*Rutgers University, Piscataway, NJ 08854*

(Dated: October 4, 2006)

We present a Raman scattering study of the  $E_{2g}$  phonon anharmonicity and of superconductivity induced self-energy effects in  $\text{MgB}_2$  single crystals. We show that anharmonic two phonon decay is mainly responsible for the unusually large linewidth of the  $E_{2g}$  mode. We observe  $\sim 2.5\%$  hardening of the  $E_{2g}$  phonon frequency upon cooling into the superconducting state and estimate the electron-phonon coupling strength associated with this renormalization.

PACS numbers: 74.70.Ad, 74.25.Ha, 74.25.Gz, 78.30.Er

High- $T_c$  superconductivity in  $\text{MgB}_2$  is known to be promoted mainly due to the boron layers<sup>1</sup>, thus the high frequency lattice vibrations of light boron atoms beneficially increase the electron-phonon coupling. The  $E_{2g}$  Raman active in-plane boron vibrational mode contributes significantly to superconductivity; this fact is reflected by the Eliashberg function  $\alpha^2 F(\omega)$  peaking in the same frequency range where a high phononic density of states is accounted for by Van Hove singularities of the  $E_{2g}$  branch in the  $\Gamma$  and  $A$  points of the Brillouin zone (BZ)<sup>2,3</sup>. The reason the  $E_{2g}$  mode plays a prominent role in the superconducting (SC) mechanism is that the mode strongly couples to the  $\sigma$ -type states of the boron plane as can be seen from the basic geometry of the electronic configuration<sup>4</sup>.

Raman spectra exhibit unusually broad linewidth of the  $E_{2g}$  mode<sup>5,6,7</sup> which has been the subject of numerous speculations. While high impurity scattering in earlier low quality samples has been suggested as one of the possible reasons, this mechanism can be readily excluded with recent high quality single crystals. The two remaining contributions to the  $E_{2g}$  phonon rapid decay are (i) strong electron-phonon coupling and (ii) multiphononic decay (subsequently referred to as *anharmonicity*). The relative importance of the electron-phonon coupling and anharmonicity in this matter is under intense debate. On one hand a density functional theory calculation asserts that the anharmonic contribution to the  $E_{2g}$  phonon linewidth is negligible ( $\sim 1$  meV)<sup>8</sup>. On the other hand analysis of the phonon self-energy in the long wavelength limit shows that the  $\sigma$ -band contribution to the phonon decay is vanishing<sup>9</sup>. Thus, even when contributions of the spectral weight of  $\alpha^2 F(\omega)|_{\omega < \omega_{E_{2g}}}$  to the damping of the  $E_{2g}$  phonon are accounted for,<sup>10</sup> the experimentally observed linewidth of 25-35 meV at low temperatures<sup>5,6</sup> cannot be explained with electron-phonon coupling alone whose part in the  $E_{2g}$  mode linewidth at low temperatures amounts to about 6 meV even in such an elaborate scenario as that in Ref.<sup>10</sup>.

Raman scattering experiments have shown that the frequency of the  $E_{2g}$  mode in single crystals at room temperature is around 79 meV<sup>5,6</sup> whereas theoretical calculations systematically underestimate this value by about 10 meV<sup>3,8</sup>. It has been suggested that if the  $E_{2g}$  band around the  $\Gamma$ -point is anharmonic then the  $E_{2g}$  mode frequency is increased by the missing amount to match the experimentally observed

value<sup>13,14</sup>. In addition, the experimentally observed  $T_c$  and the reduced isotope effect<sup>12</sup> can only be reconciled within anisotropic strong coupling theory if the  $E_{2g}$  mode anharmonicity is explicitly included<sup>4,11</sup>.

Since the  $E_{2g}$  mode is responsible for a significant part of the SC pairing a renormalization of the mode frequency upon entering into the SC phase is expected. Moreover, it was predicted that the mode renormalization along the  $\Gamma - A$  direction of the BZ is particularly strong<sup>13</sup>. The temperature dependence of phonon dispersions has been studied by inelastic x-ray scattering, however, the expected self-energy effects have not been demonstrated<sup>8,15</sup>. In earlier Raman work on single crystalline  $\text{MgB}_2$  a change of line width between room temperature and  $T_c$  has been observed<sup>6</sup> but not discussed. In the experimental context it is important to notice that single crystal studies should preferably be considered as a valid gauge of  $\text{MgB}_2$  bulk properties because results from powdered, polycrystalline, ceramic, film, wire etc. samples show significant variations, especially in relation to phonon excitations (compare Refs.<sup>7,16</sup>).

In this work we provide spectroscopic information on (i) the  $E_{2g}$  phonon excitation resonance, (ii) the reasons for the mode's large linewidth, and (iii) the self-energy effects upon entering into the SC state. In particular, (i) by means of the resonant Raman excitation profile (RREP) we show that the light couples to the  $E_{2g}$  phonon *via*  $\sigma - \pi$  inter-band transition; (ii) we study the  $E_{2g}$  phonon shape as a function of temperature and fit the linewidth temperature dependence with an anharmonic decay model; (iii) we observe the  $E_{2g}$  phonon renormalization (mode hardening  $\sim 2.5\%$ ) upon entering into the SC phase.

Raman scattering from the  $ab$  surface of  $\text{MgB}_2$  single crystals grown as described in Ref.<sup>17</sup> was performed in backscattering geometry using about 1 mW of incident power focused to a  $100 \times 200 \mu\text{m}$  spot. We have collected data from two samples that are denoted as crystal  $\mathcal{A}$  and crystal  $\mathcal{B}$  when a distinction is necessary. The magnetic field data were acquired with a continuous flow cryostat inserted into the horizontal bore of a SC magnet. The sample temperatures quoted have been corrected for laser heating. We used the excitation lines of a  $\text{Kr}^+$  laser and a triple-grating spectrometer for analysis of the scattered light. The data were corrected for the spectral response of the spectrometer and CCD detector and for

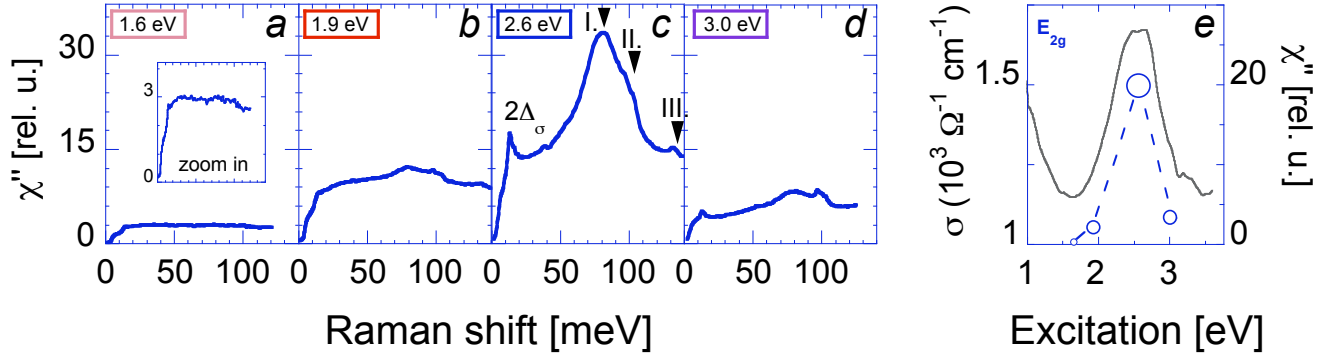


FIG. 1: (Color online) Raman response function from crystal  $\mathcal{A}$  at 8 K for  $VH$  (a) and  $RL$  (b-d) polarizations corresponding to  $E_{2g}$  channel for four excitation energies between 1.65 and 3.05 eV. The spectra exhibit a broad electronic continuum, a superconducting coherence peak  $2\Delta_\sigma$ , the  $E_{2g}$  boron stretching phonon mode (I) and two-phonon scattering bands (II - III). The comparison of  $ab$ -plane optical conductivity (Ref.<sup>19</sup>) and the  $E_{2g}$  mode intensity is shown in panel (e). The size of the symbols is proportional to the ratios of mode to electronic background intensity.

optical properties of the material at different wavelengths as described in Ref.<sup>18</sup>.

The point group associated with  $\text{MgB}_2$  is  $D_{6h}$ ; subsequently, polarized Raman scattering from the  $ab$  surface couples to two symmetry channels:  $E_{2g}$  and  $A_{1g}$ . The corresponding symmetry channels can be resolved if the appropriate light polarization is chosen for the in- and out-coming photons; in this work only the  $E_{2g}$  symmetry channel will be discussed. We denote by  $(\mathbf{e}_{in}\mathbf{e}_{out})$  a configuration in which the incoming/outgoing photons are polarized along the  $\mathbf{e}_{in}/\mathbf{e}_{out}$  directions. In the  $VH$  configuration the light is linearly polarized with vertical ( $V$ ) or horizontal ( $H$ ) directions chosen perpendicular or parallel to the crystallographic  $a$ -axis. The "right-left" ( $RL$ ) notation refers to circular polarization:  $\mathbf{e}_{in} = (H - iV)/\sqrt{2}$ , with  $\mathbf{e}_{out} = \mathbf{e}_{in}^*$  for the  $RL$  geometry. Both the  $RL$  and the  $VH$  polarization combinations select the  $E_{2g}$  representation.

In Fig. 1 we show the Raman response as a function of excitation energy sampling laser lines  $\lambda_L = 752.5, 647.1, 482.5,$  and  $406.7$  nm. We chose steps in excitation wavelengths to resolve the broad band at around 2.6 eV in the  $\text{MgB}_2$  optical conductivity<sup>19</sup>.

Typical Raman features of  $E_{2g}$  symmetry from a  $\text{MgB}_2$  single crystal are shown in Fig. 1 c where phonon modes are designated with arrows. We see that the  $E_{2g}$  mode at  $\sim 80$  meV (I.) dominates the Raman response. In addition two-phonon scattering peaks II. and III. corresponding to flat portions of the phonon dispersion curves at half the frequency of the respective peaks are also observed<sup>8,20</sup>. Finally the spectra exhibit a strong electronic continuum with a SC pair breaking peak at 13.6 meV corresponding to twice the value of the SC gap in the  $\sigma$  bands<sup>6</sup>. The evolution of the pair breaking peak with cooling below  $T_c$  is shown in insets of Figs. 2 a and 3 a.

The RREP relates Raman scattering intensity to the interband transitions seen in the optical conductivity  $\sigma(\omega)$ . It is particularly helpful in the visible range because the interband contribution to  $\sigma_{ab}(\omega)$  contains a pronounced band around 2.6 eV<sup>19,21</sup>. In Fig. 1 a-d we show that the intensity of Raman response is in resonance with the 2.6 eV band (Fig. 1 e).

We note that the ratio of the  $E_{2g}$  mode intensity to the strength of the electronic background is also largest around the 2.6 eV excitation. The Raman intensity of the  $E_{2g}$  mode is plotted along the right y-axis in Fig. 1 e as a function of excitation while the mode intensity to background ratio is represented by the size of the data symbols in the plot. The 2.6 eV peak in optical conductivity is associated with the  $\pi \rightarrow \sigma$  electronic transitions in the vicinity of the  $\Gamma$  point and  $\sigma \rightarrow \pi$  transitions in the vicinity of the  $M$  point of the BZ<sup>1,22,23</sup>. The RREP indicates that coupling to the  $E_{2g}$  mode is realized via the  $\pi \leftrightarrow \sigma$  interband transition. The strongly resonant behavior of the  $E_{2g}$  mode places experimental restrictions on how this mode should be investigated.

In Fig. 2 a Raman spectra for the SC state (zero field) and normal state ( $H > H_{c2}$ ) are juxtaposed, demonstrating the effect of magnetic field applied parallel to the  $c$ -axis at 8 K. The  $E_{2g}$  phonon mode hardens below the SC phase transition along with a slight renormalization of its linewidth. At the same time a SC pair breaking peak at 13.6 meV appears indicating the presence of the SC gap. In Fig. 2 b we demonstrate how the linewidth of the  $E_{2g}$  mode monotonically narrows from room temperature down to  $T_c$ . To quantify the dependence of the  $E_{2g}$  phonon frequency and linewidth as a function of temperature and magnetic field we fitted the data with a sum of phononic oscillators and a SC pair breaking singularity on an electronic background as demonstrated in Fig. 2 a.

In Fig. 3 we evaluate the  $E_{2g}$  phonon frequency  $\omega_0(T)$  and the damping constant  $\Gamma(T)$  for both crystals  $\mathcal{A}$  and  $\mathcal{B}$  where we distinguish between the respective values for the normal and SC states. The solid line in Fig. 3 b is a fit of the damping constant  $\Gamma(T)$  in the normal state to a model of anharmonic two and three phonon decay at one-half and one-third frequencies:

$$\Gamma(T) = \Gamma_0 + \Gamma_3[1 + 2n(\Omega(T)/2)] + \Gamma_4[1 + 3n(\Omega(T)/3) + 3n^2(\Omega(T)/3)]. \quad (1)$$

Here  $\Omega(T) = hc\omega_h/k_B T$ , with the harmonic frequency  $\omega_h = 67 \text{ meV}$ <sup>1,8,23</sup>,  $n(x)$  is the Bose-Einstein distribution function,  $\Gamma_0$  is the internal temperature independent linewidth

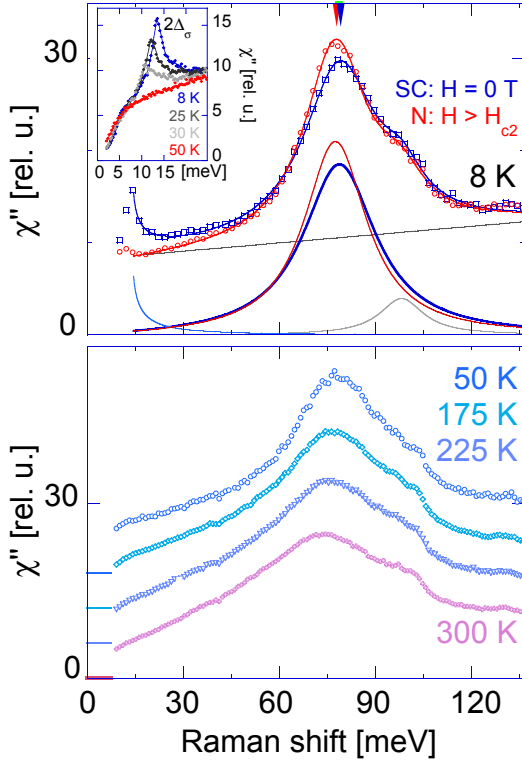


FIG. 2: (Color online) Raman response function in the  $E_{2g}$  channel for  $RL$  polarization and 2.6 eV excitation. Panel (a): Raman response from crystal  $B$  at 8 K. Spectra at zero field and 7 T are compared. Spectra are decomposed into two Raman oscillators, electronic background (linear slope), and coherence peak singularity for the SC state,  $\sim [\omega \sqrt{(\omega^2 - (2\Delta)^2)}]^{-1}$ . The arrows at the top indicate the shift of the  $E_{2g}$  mode in the transition from the SC state (blue squares) into the normal state (red circles). Inset: evolution of low-frequency Raman response with temperature across the SC transition. Panel (b): Data from crystal  $A$ . Temperature dependence of the  $E_{2g}$  phonon mode above  $T_c$ . Fit parameters to these spectra are displayed in Fig. 3.

of the phonon, and  $\Gamma_{3,4}$  are broadening coefficients due to the cubic and quartic anharmonicity. The results of the fit to this anharmonic decay model are collected in Table I. For both crystals the broadening coefficients  $\Gamma_3 + \Gamma_4 \gg \Gamma_0$  and therefore the anharmonic decay is primarily responsible for the large damping constant of the  $E_{2g}$  phonon. We identify the reason for this rapid phononic decay in the phononic density of states (PDOS) peaking at 33 meV, half of the harmonic  $E_{2g}$  phonon frequency  $\omega_h$  (see Fig-s,1 a in Ref.<sup>3</sup> and Ref.<sup>25</sup>), which corresponds to the Van-Hove singularity of the lower acoustic branch (almost dispersionless along the  $\Gamma - K - M$  direction, see Fig. 3 in Ref.<sup>24</sup>). In this context the narrowing of the  $E_{2g}$  mode with Al substitution observed in Refs.<sup>5,24</sup> can be readily explained with the  $E_{2g}$  phonon branch moving to energies above 100 meV with increased Al concentration whereas the acoustic modes that provide the decay channels stay close to their original energies with high PDOS in the energy range of 25 - 40 meV<sup>24</sup>. In short, the fast decay of the  $E_{2g}$  mode is due to the unique combination of its harmonic frequency

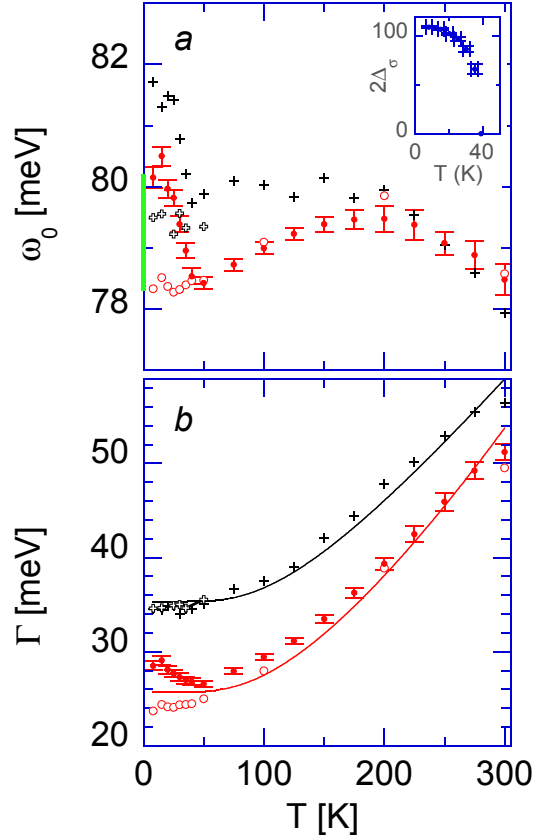


FIG. 3: (Color online) Temperature dependences for the  $E_{2g}$  phonon frequency,  $\omega_0(T)$ , (a) and damping constants,  $\Gamma(T)$ , (b) for two  $MgB_2$  single crystals  $A$  (black crosses) and  $B$  (red circles) for zero field cooling (solid symbols) and field cooling at  $8 T > H_{c2}$  (empty symbols). Solid lines are fits of damping constants  $\Gamma(T)$  in the normal state with eq. (1). The parameters from the anharmonic decay fits for both crystals are summarized in Table I. Inset shows temperature dependence of the  $2\Delta_\sigma$  coherence peak which follows from the evaluation of spectra shown in the inset to Fig. 2 a. The green bar at the  $y$ -axis indicates the  $E_{2g}$  phonon frequency renormalization upon the SC phase transition.

in the  $\Gamma$  point (67 meV) corresponding to high PDOS at half of this frequency. Thus two independent puzzle pieces; (i) the cubic anharmonicity contribution being much larger than the residual linewidth and (ii) the phonon density peaking just at the right energy to provide suitable decay channels, fit together, giving evidence that the  $E_{2g}$  phonon anharmonicity is responsible for the unusually broad linewidth of this mode. In contrast to recent theoretical suggestions<sup>8</sup> current experiment shows that the  $E_{2g}$  phonon anharmonicity in  $MgB_2$  must not be neglected. The residual linewidth  $\Gamma_0$  that we obtain from the fit to the anharmonic decay model, while small, is not in contradiction to theoretical estimates<sup>9,10</sup> of the electron-phonon decay contribution to the  $E_{2g}$  phonon linewidth.

It is worth noting that individual  $\Gamma_i$  parameters differ for the two single crystals despite the fact that both samples were grown in the same batch. The  $E_{2g}$  mode for crystal  $A$  is by about 10 meV broader than for crystal  $B$ . With  $\Gamma_0^A$  somewhat higher than  $\Gamma_0^B$  and  $\Gamma_3^A$  substantially higher than  $\Gamma_3^B$  (see Ta-

TABLE I: Comparison of  $T_c$  and the  $E_{2g}$  oscillator parameters for crystals  $\mathcal{A}$  and  $\mathcal{B}$ .

crystal	$T_c^a$	$\omega_0^{Nb}$	$\omega_0^{SCb}$	$\Gamma_0^b$	$\Gamma_3^b$	$\Gamma_4^b$	$\kappa$ (%)
$\mathcal{A}$	38.2	79.3	81.7	$4.0 \pm 1.5$	$31.4 \pm 1.2$	small	$2.8 \pm 0.5$
$\mathcal{B}$	38.5	78.1	80.5	small	$22.9 \pm 0.7$	$2.8 \pm 0.4$	$2.3 \pm 0.3$

<sup>a</sup>in K, from SQUID measurements at 2 G; <sup>b</sup>in meV

ble I) the  $E_{2g}$  mode in crystal  $\mathcal{A}$  is more anharmonic than in crystal  $\mathcal{B}$ . Accordingly the crystal  $\mathcal{A}$  mode is pushed to about 1.2 meV higher frequency at low temperatures. We note a correlation between the larger anharmonicity and slightly lower  $T_c$  in the case of crystal  $\mathcal{A}$ .

To describe the superconductivity induced self-energy effect we refer to Fig. 3 *a*. Upon cooling in zero field  $\omega_0(T)$  exhibits non-monotonic but smooth behavior down to  $T_c$ . Then at  $T_c$  it displays abrupt hardening with  $\omega_0^{SC}(T)$  scaling to the functional form of the SC gap magnitude  $2\Delta_\sigma(T)$  (Fig. 3 inset). For in-field cooling the  $E_{2g}$  phonon frequency  $\omega_0^N(T)$  remains unrenormalized. The differences between the phonon frequencies in the normal and SC states at 8 K are  $2.2 \pm 0.4$  and  $1.8 \pm 0.2$  meV for crystals  $\mathcal{A}$  and  $\mathcal{B}$  respectively. To quantify the relative hardening of the  $E_{2g}$  mode we ob-

tain the superconductivity induced renormalization constant  $\kappa = (\omega_0^{SC}/\omega_0^N) - 1 \approx 2.5\%$  (see Table I) which is much smaller than the theoretically predicted  $\kappa \approx 12\%$ <sup>13</sup>.

We estimate the electron-phonon coupling constant  $\lambda_{E_{2g}}^\Gamma$  around the BZ center using approximations adopted in Refs.<sup>26,27</sup>:  $\lambda = -\kappa \mathcal{R}e\left(\frac{\sin u}{u}\right)$ , where  $u \equiv \pi + 2i \cosh^{-1}(\omega^N/2\Delta_\sigma)$ , and obtain  $\lambda_{E_{2g}}^\Gamma \approx 0.3$ , which is smaller than the theoretically predicted values (compare  $\lambda$  up to unity in Refs.<sup>1,13,28</sup>).

In summary, we have measured the polarization resolved Raman response as a function of excitation energy, temperature, and field for MgB<sub>2</sub> single crystals. From the temperature dependence of the  $E_{2g}$  boron stretching phonon we conclude that anharmonic decay is primarily responsible for the anomalously large damping constant of this mode. For this phonon we observe a SC induced self-energy effect and estimate the electron-phonon coupling constant.

We acknowledge V. Guritanu and A. Kuz'menko for providing optical data, and I. Mazin and W. E. Pickett for valuable discussions. A. M. has been supported in part by the German National Academic Foundation and by the Lucent-Rutgers Fellowship Program.

\* Corresponding author. E-mail: girsh@bell-labs.com

<sup>1</sup> J. Kortus, I. Mazin, K. Belashchenko, V. Antropov, and L. Boyer, *Phys. Rev. Lett.* **86**, 4656 (2001).

<sup>2</sup> D. Daghero, R. Gonnelli, G. Ummarino, O. Dolgov, J. Kortus, A. Golubov, and S. Shulga, *Physica C* **408-410**, 353 (2004).

<sup>3</sup> T. Yildirim *et al.*, *Phys. Rev. Lett.* **87**, 037001 (2001).

<sup>4</sup> H. Choi, D. Roundy, S. Hong, M. Cohen, and S. Loule, *Nature* **418**, 758 (2002).

<sup>5</sup> B. Renker, H. Schober, P. Adelman, P. Bohnen, D. Ernst, R. Heid, P. Schweiss, and T. Wolf, *J. Low Temp. Phys.* **131**, 411 (2003).

<sup>6</sup> J. Quilty, S. Lee, A. Yamamoto, and S. Tajima, *Phys. Rev. Lett.* **88**, 087001 (2002).

<sup>7</sup> A. Goncharov *et al.*, *Phys. Rev. B* **64**, 100509 (2001).

<sup>8</sup> A. Shukla *et al.*, *Phys. Rev. Lett.* **90**, 095506 (2003).

<sup>9</sup> M. Calandra and F. Mauri, *Phys. Rev. B* **71**, 064501 (2005).

<sup>10</sup> E. Cappelluti, *Phys. Rev. B* **73**, 140505 (2006).

<sup>11</sup> H. Choi, D. Roundy, H. Marvin, L. Cohen, and G. Steven, *Phys. Rev. B*, **66**, 020513 (2002).

<sup>12</sup> D. Hinks and J. Jorgensen, *Physica C* **385**, 98, (2003).

<sup>13</sup> A. Liu, I. Mazin, and J. Kortus, *Phys. Rev. Lett.* **87**, 087005 (2001).

<sup>14</sup> L. Boeri, E. Cappelluti, and L. Pietronero, *Phys. Rev. B* **71**, 012501, (2005).

<sup>15</sup> A. Baron, H. Uchiyama, Y. Tanaka, K. Bohnen, S. Tajima, and T. Ishikawa, *Phys. Rev. Lett.* **92**, 197004 (2004).

<sup>16</sup> H. Martinho, C. Rettori, P. Pagliuso, A. Martin, N. Moreno, and J. Sarrao, *Sol. St. Comm.* **125**, 499 (2003).

<sup>17</sup> J. Karpinski *et al.*, *Supercond. Sci. Tech.* **16**, 221 (2003).

<sup>18</sup> G. Blumberg, R. Liu, W. Dabrowski, M. Klein, W. Lee, D. Ginsberg, C. Gu, B. Veal, and B. Dabrowski, *Phys. Rev. B* **49**, 13295 (1994).

<sup>19</sup> V. Guritanu, A. Kuzmenko, D. van der Marel, S. Kazakov, N. Zhigadlo, and J. Karpinski, *Phys. Rev. B* **73**, 104509 (2006).

<sup>20</sup> Referring to Fig. 3 from Ref.<sup>8</sup> we read the phonon dispersion to find that the two-phonon peak *II* results from the  $A_{2u}$  branch that is mostly flat all the way along the  $\Gamma$ -A line at around 46-47 meV. The  $E_{2g}$  optical branch has a minimum in A-point at 66 meV resulting in the two-phonon scattering peak *III*.

<sup>21</sup> A. Kuz'menko *et al.*, *Sol. St. Comm.*, **121**, 479 (2002).

<sup>22</sup> V. Antropov, K. Belashchenko, M. van Schilfgaarde and S. Rashkeev, *cond-mat/0107123*.

<sup>23</sup> I. Mazin and V. Antropov; *Physica C* **385**, 49 (2003).

<sup>24</sup> K. Bohnen, R. Heid, and B. Renker, *Phys. Rev. Lett.* **86** 5771 (2001).

<sup>25</sup> R. Osborn, E. Goremychkin, A. Kolesnikov, and D. Hinks, *Phys. Rev. Lett.* **87**, 017005 (2001).

<sup>26</sup> R. Zeyher and G. Zwicknagl, *Z. Phys. B* **78**, 175 (1990).

<sup>27</sup> C. Rodriguez, A. Liechtenstein, I. Mazin, O. Jepsen, O. Andersen, and M. Methfessel, *Phys. Rev. B* **42**, 2692 (1990).

<sup>28</sup> A. Golubov *et al.*, *J. Phys. Cond. Mat.* **14**, 1353 (2002).